BILINGUAL PUBLISHING GROUP

Journal of Atmospheric Science Research

https://journals.bilpubgroup.com/index.php/jasr

ARTICLE

In Defence of the Biotic Pump

Peter P. Bunyard [1*], ***Ali Bin Shahid*** [2], ***Rob de Laet*** [3]

[1]*Independent Scientist, Bodmin, PL30 5NW, UK (Formerly at El Instituto de Estudios y Servicios Ambientales de la Universidad Sergio Arboleda (IDEASA), Universidad Sergio Arboleda, Bogotá 110311, Colombia)*

[2]*Independent Scientist, Islamabad 45730, Pakistan*

[3]*Independent Thinker, Campaigner, and Member of the Ecorestoration Alliance & Global Evergreening Alliance, Amsterdam, 1054HT, Netherlands*

ABSTRACT

The biotic pump theory of Anastassia Makarieva and Victor Gorshkov invited considerable controversy when published in 2007. Experiments carried out by Bunyard *et al.* on the relationship between airflow and water vapour condensation and employing the physics of ideal gases to determine absolute humidity and energy flows, indicate that the physical processes underpinning the biotic pump theory are correct and must play a significant role in determining regional and global weather patterns. Further evidence is given showing that the energies associated with condensation correlate with measured airflow. Given the role of the biotic pump in generating flying rivers over the Amazon Basin, deforestation can result in hydrological collapse. It can now be determined how close we are to that point in time. An annual precipitation of 1800 mm is close to the threshold when rainfall is insufficient to sustain the forests. Experiments on different types of vegetation, measuring vapour emissions as latent heat, indicate the degree to which plants cool their environment by means of transpiration. By regulating the rate of transpiration, plants respond to ambient temperature and prevent overheating. Forests in particular can help cool the Earth's surface. In conclusion, the invention of the atmospheric heat engine in 1700 illustrates the power of condensation to drive atmospheric air flows and its functioning illustrates the physics underpinning the biotic pump.

Keywords: Biotic Pump; Hydrological Cycle; Global Warming; Angiosperm Evapotranspiration

*CORRESPONDING AUTHOR:

Peter P. Bunyard, Independent Scientist, Bodmin, PL30 5NW, UK (Formerly at El Instituto de Estudios y Servicios Ambientales de la Universidad Sergio Arboleda (IDEASA), Universidad Sergio Arboleda, Bogotá 110311, Colombia); Email: peter.bunyard@btinternet.com

ARTICLE INFO

Received: 9 December 2024 | Revised: 9 January 2025 | Accepted: 12 January 2025 | Published Online: 17 January 2025

DOI: https://doi.org/10.30564/jasr.v8i1.9887

CITATION

Bunyard, P.P., Shahid, A.B., de Laet, R., 2025. In Defence of the Biotic Pump. Journal of Atmospheric Science Research. 8(1): 41–64.

DOI: https://doi.org/10.30564/jasr.v8i1.9887

1. Introduction

In 2007, Anastassia Makarieva and Victor Gorshkov published their first scientific paper on the proposition that dense cloud-forming over a continental rainforest would lead to the flow of humid air from the same latitude ocean [1,2]. The biotic pump theory, as they called the proposed phenomenon, was based on the notion that cloud-forming, resulting in precipitation, would lead to a partial pressure change such as to draw air up from the rainforest surface. The air, replacing that drawn-up to the clouds, would flow in as a low-level stream from the ocean [3]. The theory depended on evapotranspiration from the rainforest surpassing, even by an order of magnitude, the evaporation over the surface of the sea, such that a pressure gradient, in favour of the forested-land, would form between the land and the ocean.

In the example of the Amazon Basin, Makarieva and Gorshkov declared that the Trade Winds, flowing from Africa in both hemispheres, were pulled in by the biotic pump, and that, as a consequence, rainfall was maintained over the spread of the South American continent, from the Atlantic Coast of Brazil, to the Andean foothills 3,000 kilometres to the West. In the 1980s, Eneas Salati in Brazil showed from isotopic studies that forest transpiration over the Brazilian Amazon, combined with the flow of humid air in the Walker Circulation, maintained rainfall at average levels above 2,200 millimetres a year right across the Basin [4]. In effect, the distance from evaporation to precipitation amounted to approximately 600 kilometres, indicating a five-fold recycling across the Brazilian Amazon. Of the annual rainfall of 2,250 mm, 1,370 mm resulted from transpiration and 880 mm from the Trade Winds [5].

According to Makarieva and Gorshkov, widespread deforestation would result in the weakening of the Trade Winds such that the partial pressure gradient would become stronger over the ocean than over the land. Consequently, the flow of surface air would, in the case of the Amazon Basin, be from West to East and therefore diametrically opposed to that when the continental surface was covered with abundant, contiguous rainforest. The subsequent drying out of the continent would further weaken the Trade Winds [1].

General Circulation Models predict a 12 to 15 per cent reduction in precipitation in the western reaches of the Amazon Basin were widespread deforestation to take place. If so, the central to western Amazon would convert to savannah [6–8]. Such models fail to include a biotic pump and, according to Makarieva and Gorshkov, underestimate significantly the reduction in rainfall. On the basis that the biotic pump had failed because of deforestation, the rainfall over the western reaches of the Amazon, for instance, over the equatorial Amazon of Colombia, would reduce to less than 20 mm per year, the indication being that the transformation would not be to savannah but to the most arid of deserts [1,9–13].

Following the publication of the original paper in 2007, the climatological community, with rare exception, denied the existence of a biotic pump, suggesting instead that latitudinal differences in temperature combined with the Coriolis Force were the prime components in driving the East-to-West Trade winds [2,14].

But what if the physics underpinning the biotic pump theory, as described by Makarieva and Gorshkov, could be experimentally tested? Consequently, Peter Bunyard devised a chamber with a 4.5-metre square dimension and a width of 1-metre (**Figure 1a, 1b**). With an average air density of 1.2 kilograms per cubic metre, the enclosed air in the structure amounted to 24 kilograms. A double layer of cooling coils, taking up a total volume of 0.00193 cubic metres was attached to an outside industrial refrigerator, thereby providing sufficient cooling to bring about condensation in the small parcel of air surrounding the coils (**Figure1c**). If the condensation caused the air at that point to move, then another parcel of air would be cooled and the process would continue as long as the refrigeration was switched on [15,16].

Using fundamental ideal gas physics and with sensors to measure barometric pressure, relative humidity and temperature, the absolute humidity could be determined in grams of water vapour per cubic metre and per kilogram of humid air (*q)* as could the pascal pressure change as a result of condensation. More than 100 experiments were carried out, as published [15–17]. However, a new assessment, as presented below, of the rate of condensation, using the per second change in the partial pressure of water vapour (hPa), provided results that showed the tight correlation between airflow and condensation, as a physical reality.

Figure 1. Airflow Measurement under Cooling: (a) Experimental Setup, (b) The Structure, (c) Cooling Coil Configuration ©Peter Bunyard [15,16].

How much air was cooled per second depended on the rate of condensation and the resulting airflow. With no condensation there was no measurable airflow, even though the air at the cooling coils showed a temperature reduction of 10º C and a gain in density of 0.05 kilograms per m^3 [15, 16].

The numbers obtained from the physics were as if the volume of air undergoing cooling per second had the dimensions of one cubic metre. Given the small, relative volume of the cooling coils (0.00193 cubic metres), the actual volume of air being cooled per second was obviously far smaller, by a factor that could be readily calculated from the actual gram-quantity of rain collected, compared to that calculated from the ideal gas equations that assumed the volume encompassed one cubic metre [15,16,18].

The equations and methodology used are clearly shown in the published article [3,4,16].

In revising the experimental data for the purposes of this review, we discovered that the rate of condensation, as derived from the change in the partial pressure of water vapour, as well as from the ratio 0.17/2.5 of the latent heat energy, correlated significantly with the actual anemometer-measured airflow. Inasmuch as the same fundamental physics of condensation occurs during cloud-forming, we conclude that the biotic pump should be elevated from theory to principle.

Furthermore, we have adapted the methodology employed in the above experimentation to quantify the cooling from evapotranspiration in a variety of plants when exposed to differing weather conditions, with the experiments taking place outside and in a conservatory. Our initial findings indicate that, under direct sunlight and temperatures of 30º C, vegetation can bring about a cooling of 10º C or more per square metre of surface.

The quantification of vegetative cooling of the associated surface, from our new run of experiments, provides empirical evidence that recovering degraded lands and in particular tropical humid rainforests will bring about a significant reduction, by as much as 1º C, in global warming.

On the basis that the biotic pump is essential for the widespread watering of the Amazon Basin rainforests, we have studied the threshold when deforestation leads to a failure of the biotic pump and consequently a breakdown in the hydrological cycle such as to cause further forest die-back. The severe droughts of 2023 and 2024 which severely affected the Amazon Basin give credence to the notion that global warming and deforestation have combined to reduce the potency of the biotic pump.

2. Materials and Methods

The physics of ideal gases and in particular the Clausius-Clapeyron equation, provides the means to determine the saturation partial pressure of water vapour in the atmosphere. Multiplication by the relative humidity, gives the actual partial pressure of water vapour at that moment in time. The partial pressure change in pascals as water vapour (ppwv) condenses, can be viewed as kinetic energy, with each gram of condensation bringing about a 0.17º C reduction of temperature in 1 kilogram of air as it expands into the locus of condensation [18,19]. Condensation also releases latent heat as infrared radiation and, in an ideal adiabatic situation, the latent heat energy released as one gram of water vapour condensed, would heat one kilogram of air by 2.5º C [19]. Although the two energies are wholly different in nature, with the first being an implosive force

as a result of 1,200-fold contraction as water vapour transforms to liquid, and the second the result of latent heat IR radiation, it so happens that the 0.17/2.5 ratio of latent heat in energetic terms (watts) is exactly equal to the partial pressure change in pascals. It is an error to subtract 0.17º C from 2.5º C in the belief that, by so doing, the two distinct energy forms are properly accounted for.

As detailed in the two published papers [15,16], judiciously placed hygrometers, thermocouples, barometric sensors, and a 2-D anemometer provided the data for a physics-based analysis of water vapour flows, using Excel spreadsheets. Precisely the same methodology and physics is employed in determining the surface cooling power of vegetation.

Taking his cue from classical physics, Bunyard showed that the experimental data lent itself to determining that three distinct but related equations could be used to calculate the energy associated with the implosion of air to fill the partial vacuum as water vapour condensed [19]:

1. The reduction in partial pressure in pascals/time to give the result in watts.

2. The ratio 0.17/2.5 of latent heat/time to give the same result in watts.

3. The reduction change in local temperature from the expansion of air multiplied by the heat capacity of dry air (1000 ΔT_v) to give the same result in watts.

Each kilogram of condensed water vapour will have a latent heat value of 2.258 megajoules if it transforms to liquid and to 2.5 megajoules if from vapour to ice. Therefore the 2.5º C increased temperature of 1 kg of air from the 1-gram condensation can be determined from the equation (1), where C_p is 1000 joules per kg dry air. Equation (2) provides the temperature reduction of 0.17º C in one kg of the air surrounding the locus of condensation of 1 gram of water vapour. Rather than focussing on the temperature change, ΔT_v, we must recognise the implosion energy, from water condensation, as being practically instantaneous and forceful [19].

$$\Delta T = {}^{Lm}/_{C_p} \quad (1)$$

$$\Delta T_v = 0.621\ \Delta q\ T \quad (2)$$

where L is latent heat, m is the mass of water vapour/liquid and C_p is the heat capacity of I kg of dry air (1,000 Joules). ΔT_v (the change in temperature, Kelvin) can be derived from the equation $0.621 * \Delta q * T$, where 0.621 is the molecular weight ratio of water vapour to air (18/28), Δq is the net change in absolute water vapour humidity (kg water vapour to kg humid air) as condensation takes place and T is the temperature at that moment in Kelvin [19].

Employing the above equations in the experiments, and taking into account the adjustments required for the factor difference between the metric volume of 1 cubic metre and the actual volume, the three methods of obtaining the energy involved in the air implosion are seen to coincide perfectly, as expected. Moreover, calculations of the likely air flow around the entire chamber, 18 metres in distance, concord admirably with the actual airflow measured with a 2-D ultrasound anemometer.

The equation to bear in mind is:

$$W_s = \Delta Pa / \Delta t\, m^3 = 1{,}000\ \Delta T_v\, m^3 = 0.17\ Lg\ m^3 / 2.5\ t \quad (3)$$

3. Results

In reviewing the experiment, which Bunyard undertook on 4^h June 2018 (**Figure 2**), we show, as predicted from the physics, that the implosion energy in watts from the pressure pascal change and from the *Latent Heat Ratio* (0.17/2.5) coincide perfectly, as to be expected (Left-hand Y-axis). The right-hand Y-axis gives the anemometer readings. Three refrigeration cycles have been carried out and each time, after a short, expected delay, the circulating airflow corresponds to the implosion energy, using the equation: *Watts = 0.5 airmass* velocity,* v^2 and accounting for the 24 kg of air enclosed in the chamber. The actual air velocity around the chamber matches well the calculated peak airflow of 0.2 metres per second.

We emphasize that the use of the *Latent Heat Ratio* (LHR) means that rainfall patterns provide an historic measure of the dynamics of pressure change from condensation and subsequent airflow.

Even though the experiments were carried out some years ago, the **Figures 2-7** have not been published before. The per second change in the partial pressure of water vapour generates the peaks in the following graphs, **Figures 3, 4 and 5.** In order to conform to the increase in airflow, the peaks are inverted inasmuch as they represent a reduction in pascals and not a gain.

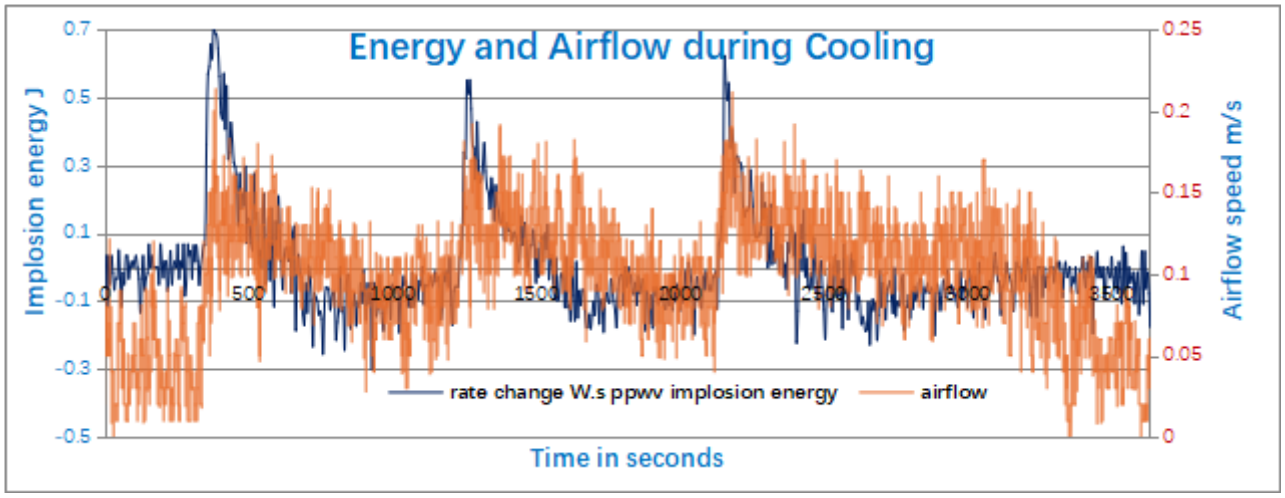

Figure 2. Experiment 4th June 2018. Left-hand Y-Axis, Using the Latent Heat Ratio to Calculate the Partial Pressure Change W.s. Right-hand Y-Axis the Corresponding Airflow (m/s). X-Axis is Time in Seconds. Three Refrigeration Cycles, Each Lasting one Minute with 5 Minutes-Interval Between.

Note: The use of the 0.17/2.5 *latent heat ratio* for calculating the implosion energy provides an unique way to evaluate the partial pressure change and consequent airflow. In essence, it means that the rate of rainfall over a region in millimetres per second will correspond closely to the average change in partial pressure of condensing water vapour when rain-clouds form. As an example, the Milton Hurricane of early October 2024, which passed over Florida, deposited 840 kilograms of rain in 24 hours. The hurricane had weakened at this stage in its progress and assuming that some 10 grams of rain were deposited every second per square metre, the implosion energy using the above ratio amounts to 1,535 watts per second or 15.35 hectopascals reduction per second in atmospheric pressure. The average (and not the peak) resulting airflow can be determined as 200 kilometres per hour or 125 mph. Were the latent heat release on condensation to be the cause of the winds, rather than implosion, the average windspeeds would be astronomically high at 765 km per hour, or 480 mph.

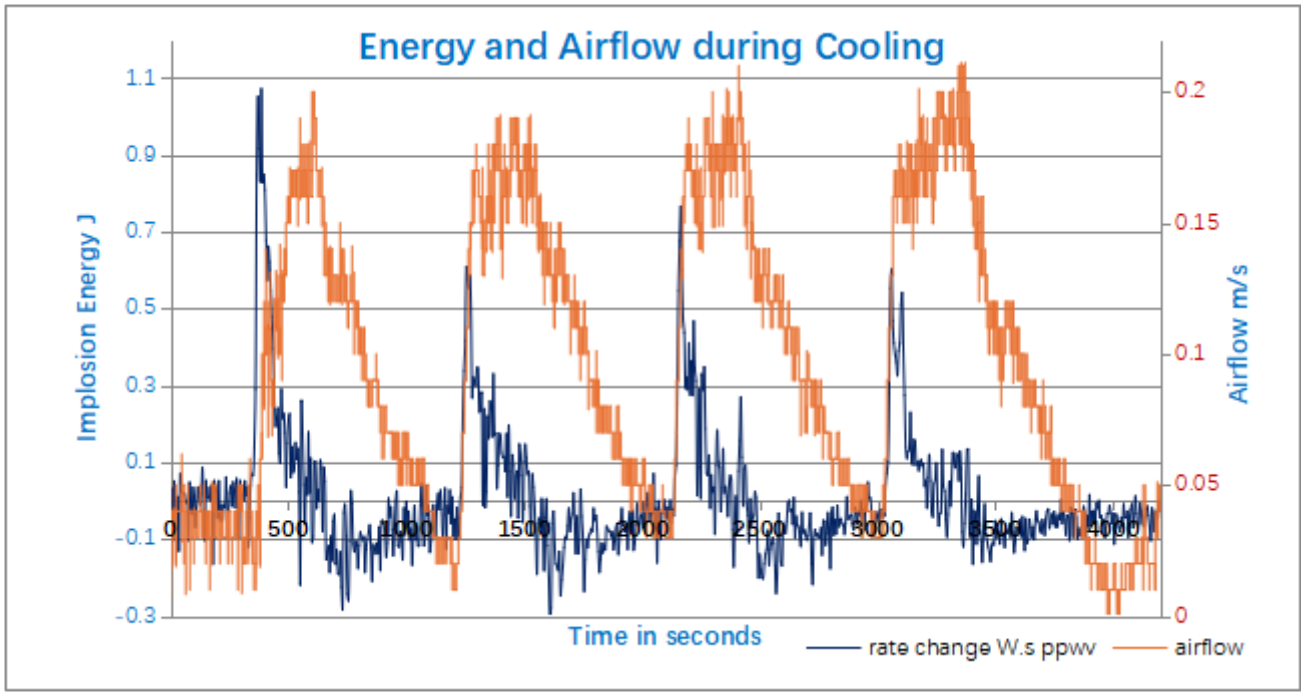

Figure 3. Experiment of 27th June, 2016. Partial Pressure Change W.s (Left Axis, W.s) versus Airflow Speed (Right Axis, m/s). Four Refrigeration Cycles.

Note: The majority of experiments indicated a flow of air down from the cooling coils, hence clockwise, as seen in **Figures 2 and 3.** But by no means all experiments resulted in a clockwise flow. On the contrary, proportionately some 10 to 15 percent of 100-plus experiments showed an anticlockwise flow. In such cases, brought about by the dynamics of the pressure, relative humidity and temperature of the enclosed air (Cornish air), the upward airflow, pushing against gravity, generally showed a less-graphically clean form than in experiments with clockwise flow.

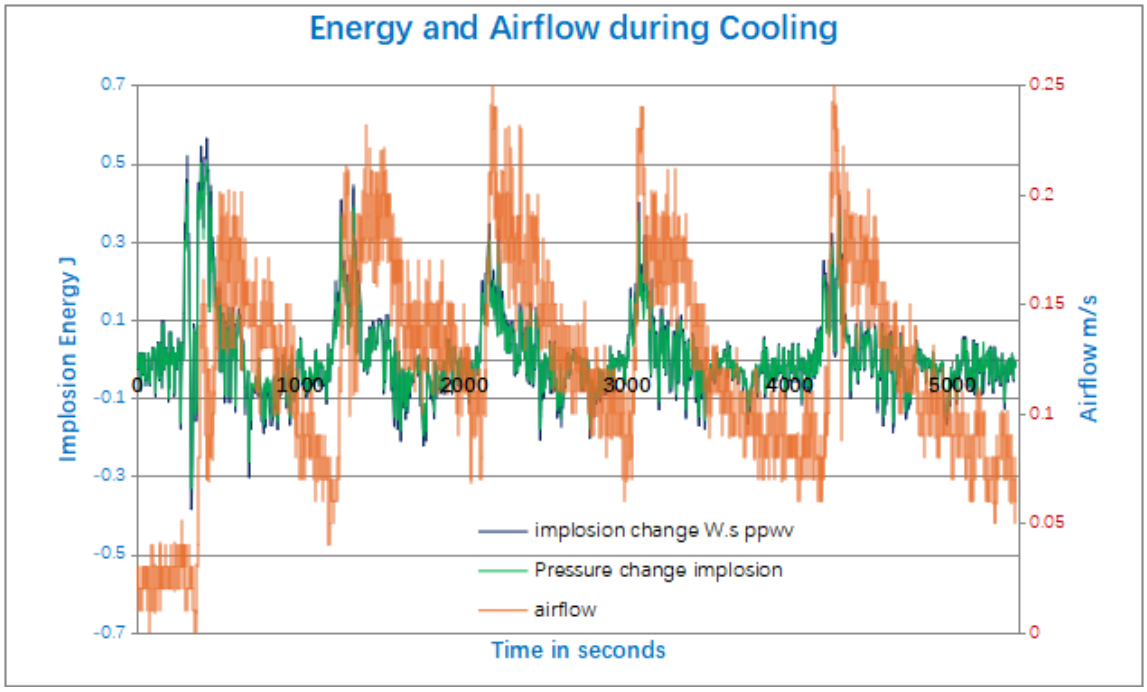

Figure 4. Experiment 27th April, 2007. Pascal Change and Use of Latent Heat Ratio (Left Axis, W.s) versus Airflow Speed (Right Axis, m/s). Refrigeration Cycles.

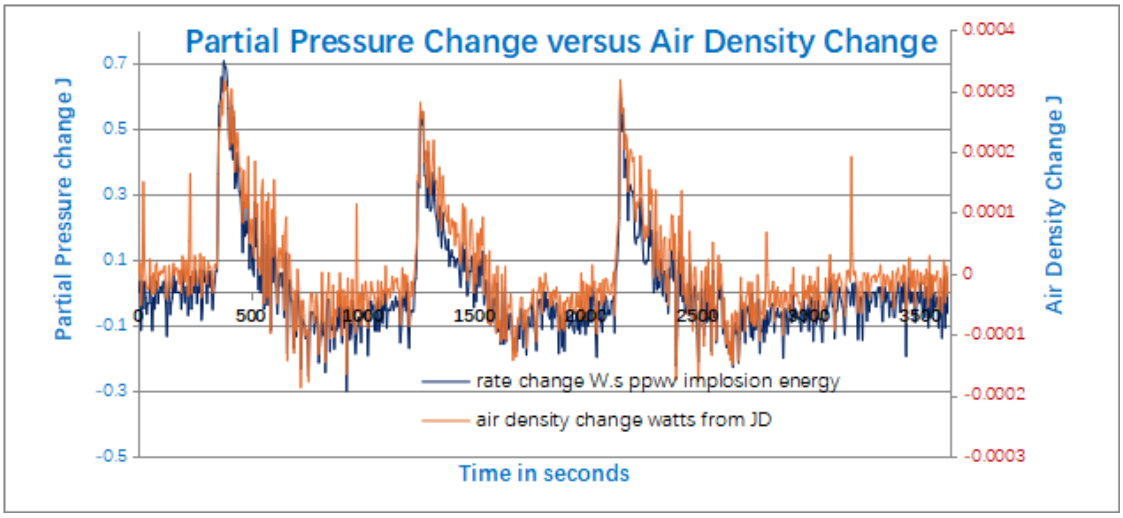

Figure 5. Experiment 4th June, 2018. Pascal Change (Left Axis, W.s). Air Density Change (Right Axis, W.s).

Below, **Figure 4**, an anticlockwise airflow showing a strong correlation between the upwards flow and the 5 refrigeration cycles. The left-hand Y-axis is of the latent heat ratio and the pascal change with the Two curves coinciding precisely.

As seen in **Figure 5**, one important finding from the experiments was that the air-density change in kilograms per cubic metre was gravitationally three orders of magnitude weaker in energetic terms (Watts/s) than the implosion energy from the partial pressure change. Therefore, the air-density change during the refrigeration cycles played a minimal role in the airflow. At best, the slight change may have encouraged the observed preferred clockwise directionality of the airflow. **Figure 5** is the experiment from June 4, 2018, where the change in air density is 2,000 times weaker in terms of energy (watt-seconds) than the change in partial pressure (see **Figure 2** for comparison).

Confirmation of the non-role of air-density change was obtained from experiments in which very little condensation occurred. See **Figures 6 and 7**. Under those

circumstances, the air-temperature reduction at the cooling coils of more than 12º C and the air-density change did not result in a correlated airflow. An important aspect of the experiments concerned the role of latent heat release on water vapour condensation. Latent heat, on release, has an energy content 15 times greater than the energy used by the air surrounding a locus of condensation. However, the clockwise flow of air in the majority of experiments, indicates that the warming associated with latent heat release is completely nullified by the cooling coil refrigeration. In that vein, the experiment of 27th June, 2018 shows a significant temperature reduction of the air at the cooling coils, but the partial pressure change is relatively small at 0.04 watts at the peak of the two refrigeration cycles which would give an airflow of no more than 0.06 metres per second. For the most part the airflow is flat-lining.

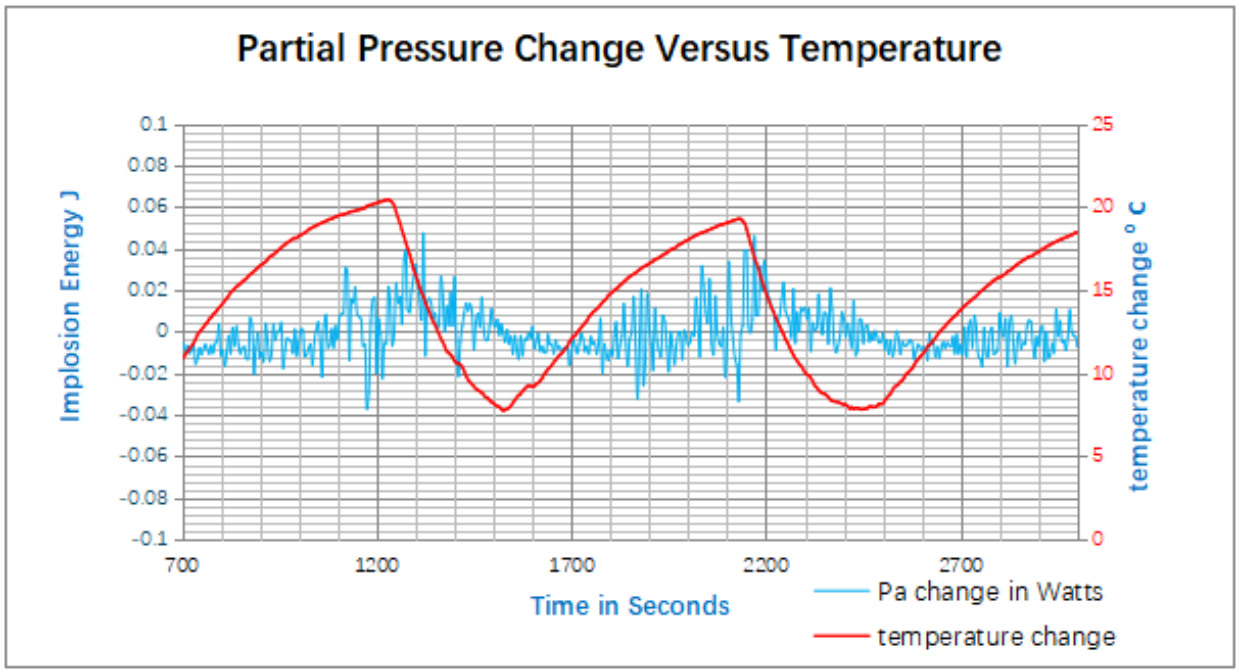

Figure 6. Experiment 27th June 2018. Pascal Change (Left Axis, W.s) versus Temperature Change (Right Axis, º C).

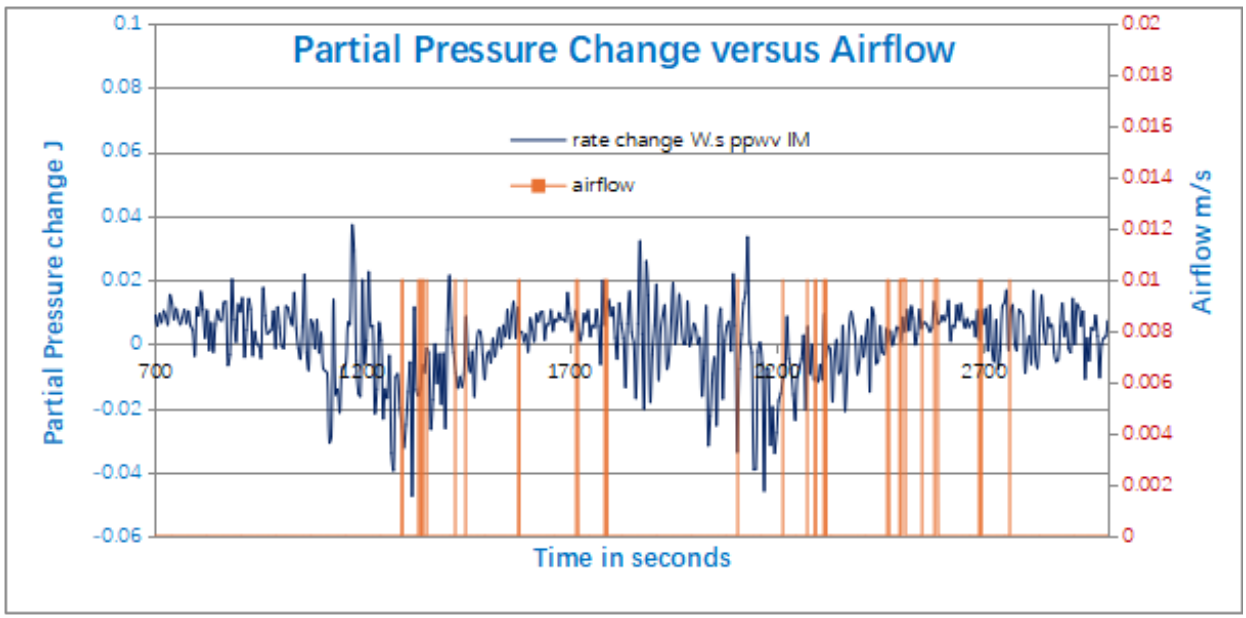

Figure 7. Experiment of 27th June, 2018. Partial Pressure Change (Left Axis, W.s) Versus Airflow (Right Axis m/s).

3.1. Rainfall Recycling

From studying the proportion of deuterium and oxygen-18 isotopes in rainwater carried by the airflows from the tropical Atlantic Ocean to the western reaches of the Amazon Basin, some 3,000 kilometres inland, Eneas Salati and his colleagues determined that the rain was recycled at least five times across the expanse of the Amazon Basin, the distance from evaporation to precipitation covering on average some 600 kilometres. Salati, as has been confirmed since, also found that as much as 60 percent of rainfall was re-evaporated by forest transpiration and that such evapotranspiration contributed to the watering of the rainforests further to the West [6,20].

The average rainfall over the forests of the Amazon Basin amounts to 2,250 millimeters per year. The average evapotranspiration over the Basin amounts to 1,370 millimeters per year, hence 61 percent of the rainfall, thus confirming Salati's finding of 40 years ago [20]. For each square metre, the energy absorbed per second, as latent heat, amounts on average to 98 watts, given that the annual evapotranspiration amounts to 1.37 metric tonnes of water per square metre, with each gram needing 2,257.2 joules to bring about the phase change from liquid to vapour. The solar input on average per second to the surface amounts to 240 watts per square metre. Therefore, the latent heat absorbs more than 40 per cent of the total irradiation received at the surface. When we add in the extra 40 per cent of evaporated moisture to make up the average rainfall, then the total latent heat required amounts to 161 watts per second, with the smaller portion being derived from solar evaporation which has taken place over the tropical Atlantic Ocean [20–22].

On forming rainfall clouds over the Amazon Basin, the vapour condenses and releases all the latent heat as infrared radiation. As much as 50 per cent will immediately irradiate upwards to Space [23]. The warmed-up, relatively dry air, will rise and, in cooling as it expands, will release energy into its immediate surroundings, some of which will, like before, escape to Space. Meanwhile, the warmed-up air gets carried by the high-level jet stream towards Africa, all the while cooling further and releasing its energy, such that over time, a considerable proportion, if not all, of the original latent heat will have escaped to Space [20,23].

3.2. Amazon Cooling

In references [3,5], we show that the annual latent heat export via IR radiation to Space from the 5.5 million km^2 of the legal Amazon of Brazil amounts to 2.6409 $x10^{22}$ watts. In 2024, NASA calculated the degree of global warming as a radiation imbalance per m^2 of 1.81 watts. Applied to the Earth's surface as a whole, in 2024, the total warming for the year comes to 2.91109 $x10^{22}$ watts. Therefore, to reduce global warming by 0.9 watts per m^2 would supposedly require the recovery and regeneration of 2.25 million km^2 of tropical rainforests, an area equivalent to the razing of tropical rainforests which has occurred since the end of World War 2. Our initial experiments confirm the cooling potential from evapotranspiration [23].

In terms of the biotic pump, the energies involved in condensation-implosion are considerable. Over the Brazilian Amazon (5.2 million square kilometres) they amount to 66 watts per square metre if delivered over four hours in the mid- to late-afternoon. Indeed, the implosion energy from cloud-forming over the 7 million square kilometres of the entire Amazon Basin is equivalent to the energy of one 18.6 kiloton atomic bomb going off every second [3,5,19,20], therefore 31.5 million such energy equivalent bombs over the course of one year. The resulting flow of air during 4 hours of rainfall each day is sufficient to account for the Trade Winds (Vientos Alisios) blowing over the tropical Atlantic from Africa to South America [20], namely an air current of 14 metres per second (see **Table 1**) [21].

Figure 8 indicates the consequence of deforestation on the rainfall as one passes away from the coast to the interior, as much as 4,000 km inland. When the forests of the Amazon Basin are intact, the biotic pump functions to bring moisture in from the same latitude ocean and rainfall levels are maintained right across to the Andes Mountains and beyond, in what we now know of as 'flying rivers'. With complete deforestation, the biotic pump fails and the decline in rainfall across the Amazon Basin is exponential, based on the distance x km from the coast and the distance from precipitation to evaporation, experimentally shown to be some 600 kilometres [6]. Meanwhile, general circulation models which do not account for a biotic pump, and instead take it for granted that the Trade Winds will continue to bring moisture inland from the ocean even were there no

forests, indicate a 10 to 12 per cent reduction in rainfall, in the far-reaches of the Basin. By contrast, for those climate projections which assume that without a functioning biotic pump the rains will fail, the far reaches of the Amazon Basin will turn to the most arid of deserts.

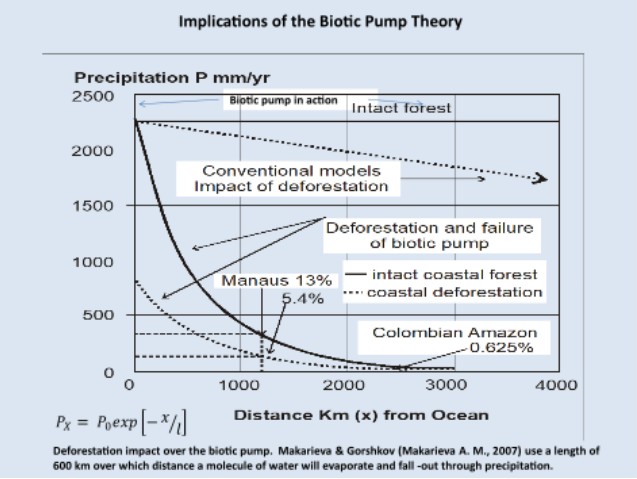

Figure 8. Precipitation (Left Axis, mm/year). Distance from Ocean (X Axis, km). Courtesy Dr. Anastassia Makarieva and Dr. Victor Gorshkov [1].

Table 1 shows how the ideal gas physics underpinning the biotic pump theory, translates into airflow speeds. As pointed out, the pressure change associated with condensation (pascals per second) can be determined from the latent heat 0.17/2.5 ratio. One gram of condensation per cubic metre per second will give an airflow of 17.5 metres per second whilst 10 grams condensed per second in each cubic metre will give an airflow of 200 km/hr.

3.3. Experiments to Show Cooling

Some 100 million years ago, when the continents were forming their current layout, came the evolution of angiosperm vegetation, with broad, veined leaves. Because of such vascularisation and access to water via their roots, angiosperm trees could transpire at a rate at least four times higher than conifers and more primordial species of trees. With contiguous, closed-canopy forests, that increase in transpiration enabled a higher rate of photosynthesis and consequently a significant increase in biomass, boosted no less by the expansion of forests deep into the hinterland of continents. It is precisely such an evolutionary change which, according to Makarieva, would have served to generate the atmospheric pressure changes we associate with the biotic pump [1,24,25].

Table 1. Rainfall Rates and Calculated Airflow Velocities.

Rainfall	Rainfall cc/s/m²	Rainfall grams g/s/m²	Latent heat 540*4.18 J/g	Latent Heat Ratio 0.17/2.5 L	Airflow velocity m/s	Airflow km/h	Airflow if rain during4 hours m/s
2,250 mm per year (e.g., Amazon rainforest)	0.07	0.07	161.12	10.96	2.34	8.43	14.04
Hurricane Milton (840 Kg/24 hrs)	9.72	9.72	21955.50	1492.97	54.64	196.72	
0.05 mm rainfall/s	50.00	50.00	112914.00	7678.15	123.92	446.11	
0.025 mm rainfall/s	25.00	25.00	56457.00	3839.08	87.63	315.45	
0.01 mm rainfall /s (Hurricane Milton)	10.00	10.00	22582.80	1535.63	55.42	199.51	
1 g water condensation/s/m²	1.00	1.00	2258.28	153.56	17.53	63.09	
0.5 g water condensation/s/m²	0.50	0.50	1129.14	76.78	12.39	44.61	
0.25 g water condensation/s/m²	0.25	0.25	564.57	38.39	8.76	31.55	

Note: cc = cubic centimetre (1 cc ≈ 1 g for water).

That important angiosperm evolutionary step helped bring down the carbon dioxide levels from more than 3,000 parts per million (by volume) to their pre-industrial concentration of 280 parts per million (ppm). Meanwhile, the biomass converted to coal, which we have been burning indiscriminately once industrialisation got underway and, indeed, which fuelled the Newcomen atmospheric heat engine at the very beginning of the industrial revolution in 1700. In general terms, over the course of 100 million years, the temperature fell *linearly* from 7ºC above pre-industrial global-average levels to that at the beginning of the industrial revolution some 250 years ago. Over the same period, carbon dioxide levels fell *exponentially*, with the greatest change occurring all those millions of years back. From **Figure 9a, b**, we see that over the past 20 million years the temperature trajectory is more or less linear with bumps, but the CO_2 atmospheric concentration shows the tail end of an exponential decline, with relatively little change (**Figure 9c**). Yet, the cooling continued over those 20 million years from 2ºC above pre-industrial levels (280 ppmv) to zero by the turn of the 19th century [26,27].

The obvious interpretation of the increase in biomass and the associated cooling was that it was the result of CO_2 uptake and the reduction in greenhouse gas concentration. Undoubtedly, such a conclusion is in part correct. However, it does not take account of the cooling brought about by a significant increase in evapotranspiration as a result of the evolution of angiosperm-dominated tropical rainforests which, over time, covered much of the continental surface. We calculate that the water-vapour transport of evapotranspired latent heat from the forest canopy to the upper troposphere and its subsequent irradiation to Space as infrared electromagnetic radiation may have brought about a cooling at least 100 times and possibly as much as 200 times greater than the cooling from biomass-forming and its role as a carbon sink [28].

The cooling power of vegetation has now been acknowledged in a recent study by Monash University Professor Yuming Guo and published in *The Lancet Planetary Health.* The wide-ranging study showed that increasing vegetation levels by 10%, 20% and 30% would decrease the global population-weighted warm-season mean temperature by 0.08° C, 0.14° C, and 0.19° C, respectively and it could have prevented 0.86, 1.02, and 1.16 million deaths, respectively [29], representing 27.16%, 32.22%, and 36.66% of all heat-related deaths from 2000 to 2019.

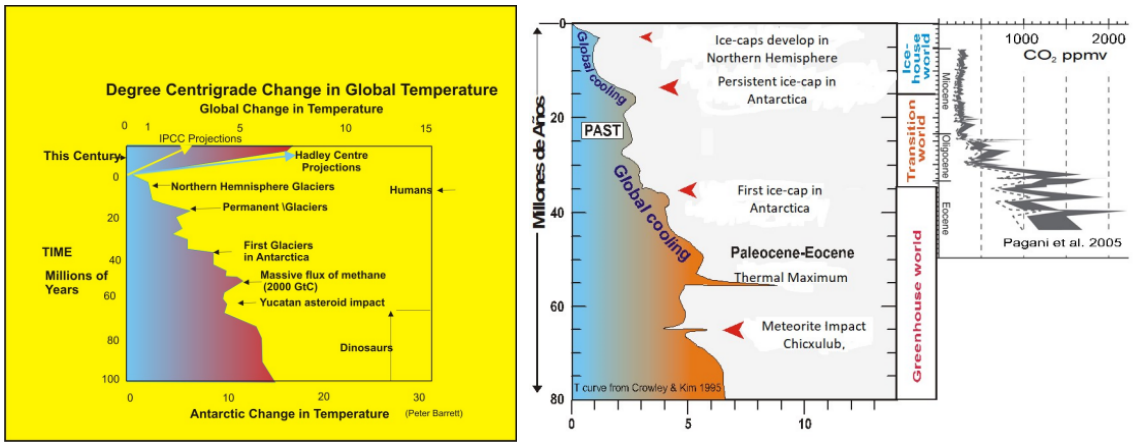

Figure 9. From Left to Middle, (**9a, 9b**) Cooling over the Past 100 Million Years Largely Follows a Linear Path, Whereas in **Figure 9c**, the Reduction in Atmospheric CO_2 is Logarithmic with a Levelling off 20 Million Years Ago**. Figure 9c**, to the right, uses the same scale for the years as in **Figure 9b** from some 50 million years ago to the present. Diagrams from Peter Barrett and Pajani, [26, 27].

3.4. Preliminary Experiments to Show the Power of Vegetation to Cool the Surface

Experiments (26h April 2025), **Figures 10** and **Figure 11**, on old pasture grass and on a tropical tree, guanábana, *Annona muricata (graviola)*, provide evidence of the cooling power brought about by evapotranspiration and the subsequent export of latent heat. Compared to artificial turf (i.e., albedo similar), the grass/graviola cool each cubic metre of air by some 10º C and 7º C, respectively, as seen in **Figure 10** (26th April 2025). That measured cooling correlates significantly with the calculated cooling, as taken from the partial pressure changes of water vapour and the absolute humidities associated with each medium (**Figure 11**). The absolute humidity associated with the non-transpiring false turf is subtracted from the transpiring pasture grass and graviola in order to calculate the net difference. All the calculations are based on the physics of ideal gases as used in the original experiments carried out on the biotic pump (published by the journal DYNA) [15–17]. As can seen in **Figure 11**, the calculated difference between grass and artificial turf amounts to the grass cooling its immediate temperature by as much as 11º C at the peaks and the graviola by as much as 8º C. The absolute humidity of the open bowl of water, when compared with the absolute humidity of the false turf, indicates that evaporation has taken place from the former, but considerably less than the evapotranspiration associated with the grass and graviola leaf.

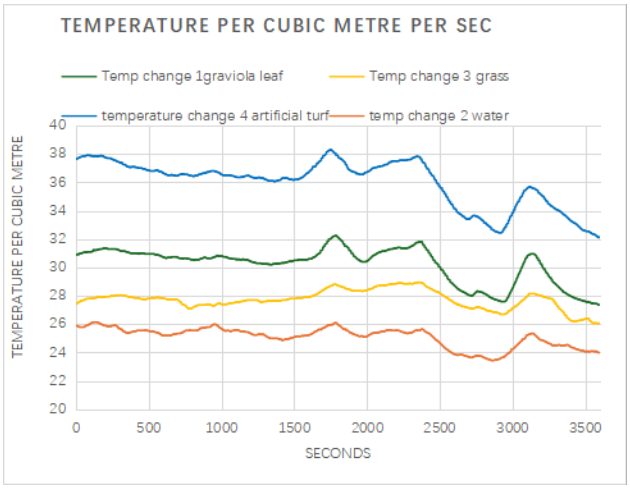

Figure 10. Experiment of 26th April 2025. The Temperature (º C) of Artificial Turf, Graviola (Soursap), Pasture Grass and Water.

In the experiment (26th April 2025, **Figures 10, 11**), tests were carried out by laying the sensor on the grass surface and on the abaxial surface of the guanábana leaf, *Annona muricata* (graviola). The room temperature, as measured by an air-control hygrometric sensor was approximately 26ºC and the temperature of the false turf, exposed to the sun to the same extent as the grass and guanabana (graviola), had a temperature of 38º C. As seen in **Figure 10**, the temperature of the grass was 2º C higher than the air measured above the water and that of graviola was warmer by around 5º C.

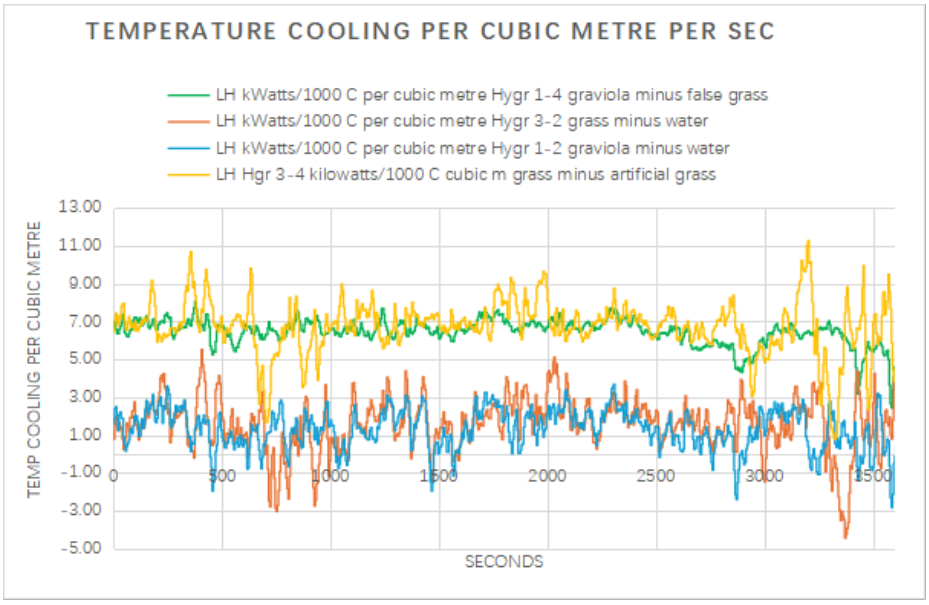

Figure 11. Experiment of 26th April 2025. (Left Axis), Cooling of Grass and Graviola by Subtracting Latent Heat kW of False Grass and of Water, then, Dividing by Cp, Heat Capacity of Air.

The experiments using pasture grass, graviola (soursop, guanábana), false turf, water, with intermittent sun provide excellent evidence that transpiration acts as an effective coolant. The increased rate of transpiration as the sun strengthens enables the plant to cool itself proportionately and the grass appears to prefer a cooler temperature to operate in than the graviola, which is a tropical plant, and best operates at temperatures of around 30º C. The rate of cooling/warming in º C per second for each of the samples is measured in kilowatts divided by the heat capacity of dry air, Cp, which, at constant barometric pressure, is 1000 joules per kg per degree Kelvin (º C). **See Equation (1).**

The results indicate that the latent heat of transpiration far exceeds the energy delivered by sunlight at any moment in time. The far higher rate of ET from the plant leaves compared to open water evaporation is because of the high pressure of liquid water in the xylem and leaf vascular system, such that when the stomata open the water under pressure bursts out as vapour into the surrounding air, just like the refrigerant substance on moving from a narrow tube to the expansion vessel of a fridge. The rapid decompression can be approximated by a Bernoulli-type expansion:

$$P_{before} + \left(1/2\ \rho v_{before}^2\right) = P_{after} + \ 1/2\ \ \rho v_{after}^2 \quad (4)$$

Where: Pbefore = pressure before P, after = pressure after, ρ = air density, vbefore = velocity before, vafter = velocity after. Flash vaporization then occurs because the local vapour pressure exceeds the boiling threshold at ambient temperature under the lower pressure. In other words: the leaf acts like a micro-scale expansion valve, with stomata serving as the outlet, turning tensioned water directly into high-velocity vapour puffs. This would explain the disproportionately high ET rates compared to open surface evaporation.

An experiment of May 22nd, 2025, (**Figures 12 and 13**), taking place at midday under bright sunshine, shows that the samples of *Geranium pratense* and the pasture sward with wild flowers (trefoil, margarita, speedwell) is transpiring and bringing the temperature down to below that of the control. The control temperature during the 4,000 second duration of the experiment rose from 30º C to 36º C, yet that of the sward with flowers rose one degree from 23.5º C to 24.7º C. The sun's intensity increased from 880 Watts per square metre to 950 Watts per square metre. Meanwhile, the temperature of the false turf, with an albedo similar to that of green leaves, rose to more than 60º C. By its emissions of transpired water vapour, the vegetation is therefore achieving a cooling of more than 30º C.

It is clear that evapotranspiration provides the plant with the means, just like perspiration, for temperatures to be maintained close to an optimal level for photosynthesis and the plant's well-being.

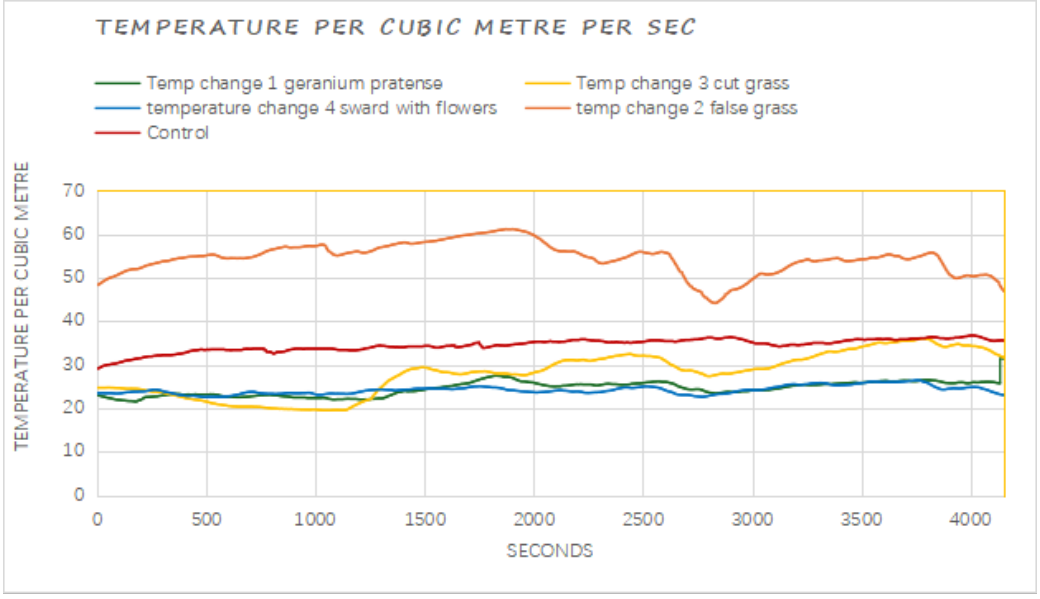

Figure 12. Experiment of 22nd May, 2025, under Bright Sunshine. The Temperature of the Grass Sward, and *Geranium* Are Below That of the Control.

On a sunny day, **Figure 13**, the capacity of the pasture sward with wild flowers to transpire at a rate which regulates the surface temperature is captured in the experiment of May 22nd, 2025. By converting the absolute humidity change into kilowatts and then dividing by the heat capacity of dry air, C_p, provides the degree of cooling in º C. Calculations of peak cooling of close to 30º C of the pasture sward and geranium indicate a good correlation with the distinct temperature difference of **Figure 12**.

Figure 13 indicates the close correlation between the rate of transpiration, as measured by changes in absolute humidity, and changes in temperature**. Figure 14**, the experiment of 11th April, 2025, shows the partial pressure changes in absolute humidity of the samples with reference to the absolute humidity of the control sample of the ambient air measured 1 metre up from the surface. The peaks and troughs as seen in the absolute humidity changes of the grass sward follow the changes in surface temperature, with the grass transpiring more vapour when the temperature increases and reducing the transpiration when the temperature falls. The outcome is a regulated temperature. In this particular experiment, the evaporation rate from the open bowl of water was close to zero resulting in the air just above the water surface having an absolute humidity close to that of the control. Indeed, whereas the contrast between the grass and water, false turf and control is considerable with peaks of 1500 Pa/Watts, that between water and the control is considerably less.

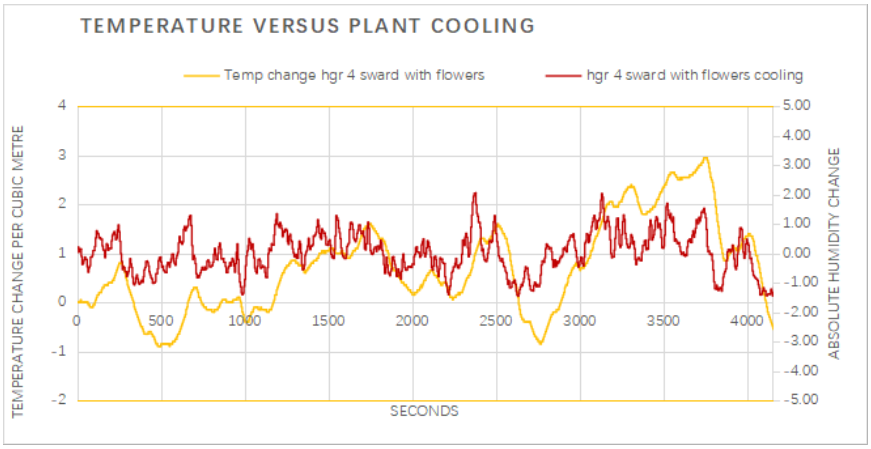

Figure 13. Experiment of 22nd May, 2025. The Temperature Change per Second (Yellow, Left Axis, º C). Absolute Humidity Change (Red, Right Axis, g/s/ Kg Moist Air).

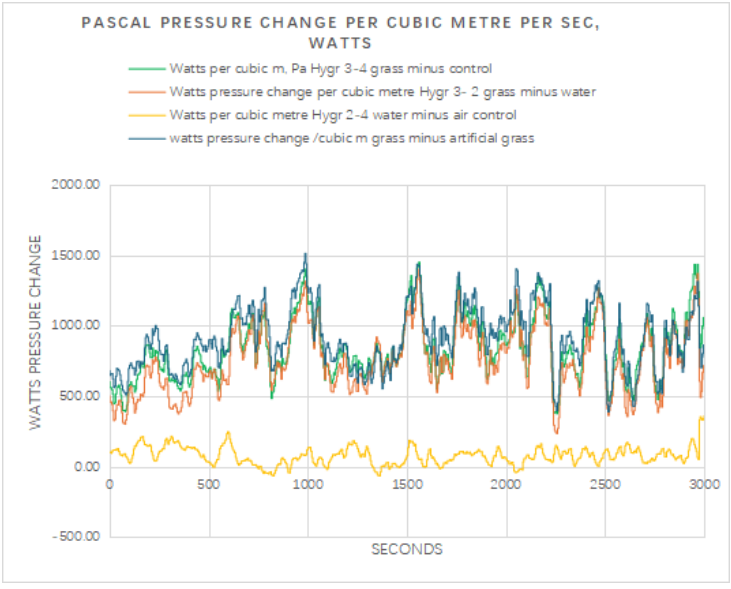

Figure 14. Experiment of 11th April (2025). Difference in the Partial Pressure of Water Vapour (Pa, W.s) Between Grass and Water, between Grass and False Turf, between Grass and Control.

Figure 15 shows the absolute humidity change per second versus the temperature change for grass. As in **Figure 13** the grass is regulating the temperature by increasing and decreasing the water vapour emissions. Peaks in temperature are immediately followed by rises in absolute humidity, with the result that the air cools. Then, as it warms again, the transpiration emissions increase. The overall result is a relatively stable temperature at a level which is optimal for plant health and growth.

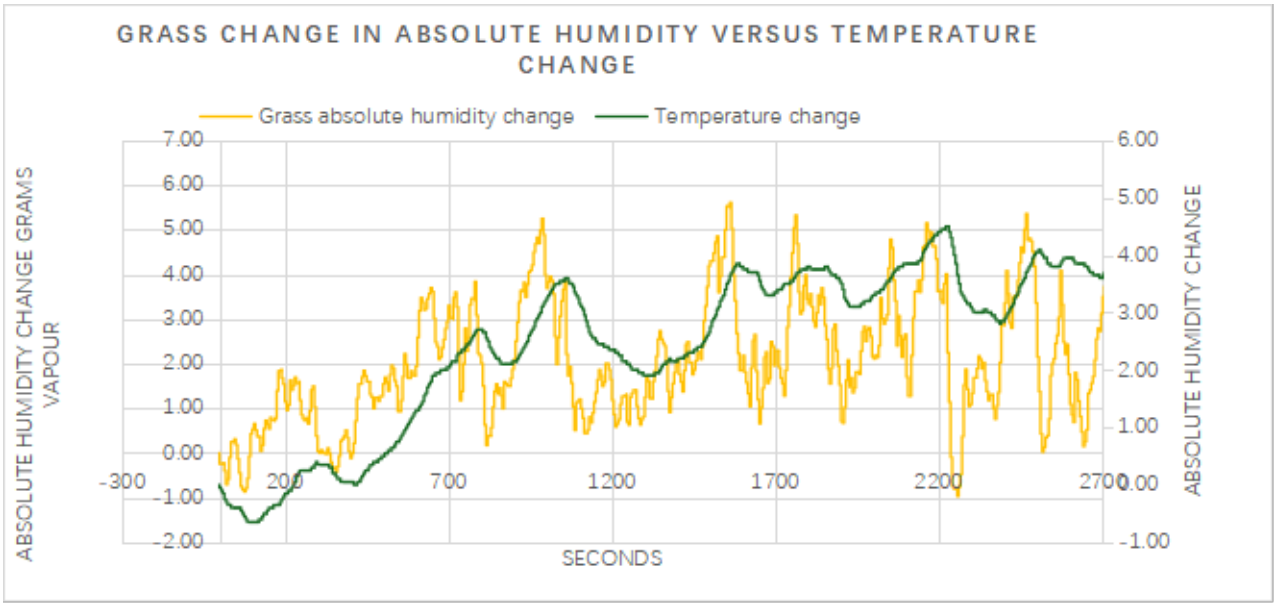

Figure 15. Experiment of 11th April, 2025. Temperature change per second º C, versus Absolute Humidity Change per second, grams per Kg moist air.

3.5. Newcomen Engine

The Newcomen engine, like the biotic pump, depended on sudden condensation combined with atmospheric pressure to drive it (**Figure 16**). Developed in 1712, it not only marked the advent of steam-powered machinery but also provided profound insights into the same fundamental thermodynamic principles which underpin the functioning of the biotic pump. Its innovative design offers a unique perspective on how localized energy transformations can drive sustained mechanical and atmospheric motion. Originally intended to pump water from mines, the Newcomen engine became a cornerstone of the Industrial Revolution, transforming industries reliant on mechanical power.

At its core, the Newcomen engine relies on the cyclic generation and removal of steam to create a vacuum that drives a piston. The process begins with heating water in a boiler to produce steam, which displaces air in the cylinder. This steam is then rapidly cooled by injecting cold water, causing it to condense. The condensation results in a dramatic 1,200-fold reduction in volume, creating a vacuum within the cylinder. Atmospheric pressure then forces the piston downward, transferring motion to a pump rod via a large overhead beam or lever. This cycle of heating, cooling, and vacuum formation repeats continuously to sustain motion.

This precise understanding of the Newcomen engine's mechanics serves as a robust analogy for atmospheric dynamics. In the biotic pump, the partial pressure reduction caused by condensation implosions creates localized vacuums that drive the horizontal movement of air, sustaining large-scale circulation patterns. Just as residual latent heat in the engine dampens the vacuum force, retained latent heat in the atmosphere disrupts the pressure gradients needed for effective airflow. Moreover, in both systems, the sharpness of the vacuum effect is paramount: the engine requires it to lift heavy loads, while the atmosphere relies on it to maintain moisture-laden winds essential for precipitation and climate regulation.

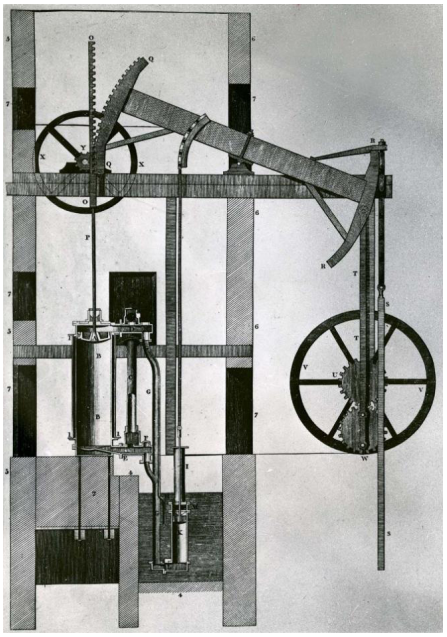

Figure 16. Newcomen Engine of 1712.

3.6. Biotic Pump Consequences

In reviewing the hydrological data from the Amazon Basin and accounting for the biotic pump, Ali Bin Shahid came to significant conclusions related to the effect of deforestation on the hydrological cycle. As stated earlier [3,5,30], the trade winds bring in approximately 40 percent of the vapour which flows across the Amazon Basin, the remainder, 60 percent, being the result of recycling [6]. On the assumption that the biotic pump is largely responsible for the trade winds flow of humid air, we find that the Amazon rainforest may cross a biome-scale tipping point not merely when a specific percentage of forest cover is lost, but rather when regional annual rainfall falls below a critical threshold of approximately 1,800 mm/year. This threshold reflects the breakdown of the forest's internal water recycling system, beyond which vast areas could transition from humid forest to degraded savannah-like ecosystems. Once annual rainfall drops below 1800 mm, the Amazon's high-humidity-adapted trees begin to die off, opening gaps in the canopy and allowing grasses to invade, especially fire-tolerant species. This transition phase can unfold over one or two decades, depending on local conditions. As tree cover diminishes, evapotranspiration declines, weakening the biotic pump and reducing rainfall further. Simultaneously, increased fire frequency accelerates forest loss and favours grasses, creating self-reinforcing feedback loops that push the ecosystem toward a savanna-like state more rapidly and finally to desert.

"Biotic pump," drawing moisture from the Atlantic Ocean deep into the continent. This critical process regulates rainfall not just within the Amazon basin but also across vast regions of South America.

At the current deforestation level of 25%, the biotic pump's efficiency has already declined to 69.9% (approximately 70%). This means that the Amazon's ability to recycle and retain moisture has been significantly compromised. Under normal conditions, the forest still receives around 2100 mm of rainfall annually, which is within a safe range to sustain its rich biodiversity.

However, climate anomalies like ENSO (El Niño Southern Oscillation) and the Pacific Decadal Oscillation (PDO) dramatically alter this balance. The 2023-24 ENSO event, coupled with a warm PDO phase, led to a sharp drop in rainfall—bringing it dangerously close to 1800 mm.

Why is 1800 mm critical?

- 1800 mm is the stress threshold for a rainforest. Below this level, the forest struggles to maintain its ecological functions.
- This rainfall deficit acts much like deforestation itself, reducing the moisture available to sustain the forest.
- In this context, climate change doesn't just "add" to deforestation—it accelerates the effects as if the forest had already lost more of its cover.

Even though there's theoretically a "buffer" of around 8% (the difference between current deforestation and the tipping point at 33.2%), this buffer is deceptive. The degradation of land along the biotic pump's pathway—from the Atlantic coast to Manaus—has already crossed critical deforestation thresholds.

This means:

- The Amazon is living on borrowed time.
- In ENSO years, the tipping point is effectively already here.
- The forest doesn't just face deforestation from chainsaws and fires—it's also under siege from invisible climate forces that mimic the effects of deforestation.

The Amazon is now in a critical tipping point scenario. The system's resilience is compromised, and every new climate shock pushes it closer to irreversible change. This isn't just a distant future risk—it's happening now.

Figure 17 presents a comparative assessment of annual rainfall and deforestation rates across three key locations in the Amazon: Belém, Marabá, and Manaus. It highlights how deforestation levels and climate stressors are driving these regions closer to—or even beyond—critical ecological tipping points.

Key Components of **Figure 17**:

1. Dark Blue Bars (Annual Rainfall):
   - Represent the average annual rainfall (in mm) for each city.
   - This shows the critical role that rainfall plays in sustaining the Amazon ecosystem.
2. Red Bars (Deforestation %):
   - Overlaying the rainfall bars, these bars represent the percentage of deforestation in each region.
   - The severity of deforestation directly influences the biotic pump's ability to recycle moisture.
3. Dashed Lines (Critical Thresholds):
   - Orange Dashed Line (2000 mm): Marks the "Warning Rainfall Threshold". Falling below this line indicates the ecosystem is under increasing stress.
   - Red Dashed Line (1500 mm): Indicates the "Critical Rainfall Threshold". Below this, forests face the risk of irreversible dieback.

City-Specific Insights:

1. Belém:
   - Rainfall: ~2900 mm/year (close to theoretical maximum).
   - Deforestation: 20%.
   - Analysis: While deforestation is significant, the region still maintains high rainfall levels due to its coastal proximity. However, this also means it's vulnerable as the "entry point" of the biotic pump.
2. Marabá:
   - Rainfall: ~1843 mm/year.
   - Deforestation: 75%—the highest among the three regions.
   - Analysis: Despite being closer to the critical rainfall threshold, Marabá still receives more rainfall than expected for such high deforestation. This is because it's still partially buffered by the Amazon's moisture system. However, it's dangerously close to tipping into irreversible decline.
3. Manaus:
   - Rainfall: ~2100 mm/year.

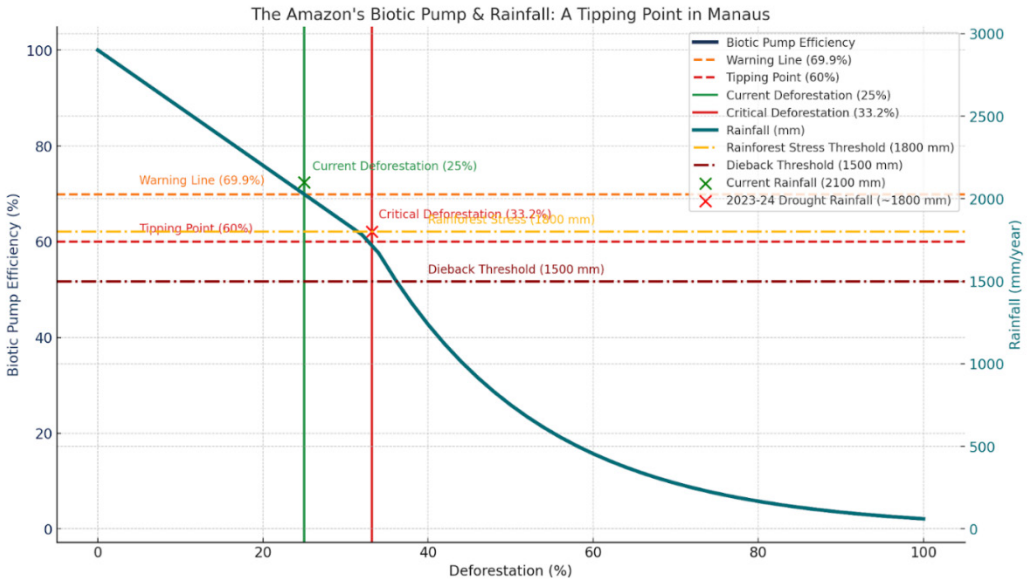

Figure 17. Annual Rainfall and Deforestation Rates Across Three Key Locations in the Amazon: Belém, Marabá, and Manaus.

- Deforestation: 25%.
- Analysis: Even though Manaus has lower deforestation compared to Marabá, the declining rainfall signals increasing stress. During ENSO events (like in 2023–24), rainfall dropped to near the warning threshold (1800 mm), suggesting that climate variability now acts as an amplifier of deforestation impacts.

Key Takeaways:

- Deforestation isn't the only threat. Climate events like ENSO and PDO act as "invisible deforestation," reducing rainfall even where tree cover remains.
- Marabá is already in crisis, with deforestation far beyond safe limits and rainfall dangerously close to the critical threshold.
- Manaus is at a tipping point. The combination of deforestation and climate anomalies has pushed it near stress thresholds, even though deforestation is "only" 25%.
- The "buffer" of remaining forest cover isn't enough to prevent tipping points during climate stress events.

Figure 18 illustrates that the Amazon is not a linear system. While deforestation rates are critical, climate variability accelerates ecosystem collapse. We're not just approaching the tipping point—in some areas, we've already crossed it. **Figure 17** highlights the Amazon's shrinking ability to recycle moisture, which in turn affects rainfall patterns both locally and across the continent.

At the historical maximum, ET reached 1370 mm/year, efficiently recycling 50–70% of rainfall with an 880 mm/year Atlantic inflow. However, the current situation paints a stark contrast. As of 2024, with 23.7% forest loss, the Amazon has already experienced a 30% rainfall deficit and an annual water loss of 2,273 km³. This decline is not solely due to deforestation—climate events like ENSO and extreme droughts have amplified the crisis.

Key observations include:

- ENSO Impact: Equivalent to an additional 5% deforestation, reducing ET without actual tree loss.
- 2023–24 Drought Impact: Functionally adds the stress of ~8% extra deforestation, pushing the system closer to critical thresholds even before reaching actual deforestation limits.
- Heat Waves (2023–24): With canopy temperatures soaring to 41°C, these events significantly reduced ET, exacerbating water stress beyond what deforestation alone would predict.

The critical threshold is marked at 33.2% forest loss, where ET drops precipitously, risking potential system collapse with 3,182 km³ of annual water loss. The alarming takeaway is that climate stressors are acting as accelerants, effectively "skipping" us forward on the deforestation curve. Even though we're at 23.7% forest loss, the compounded effects of ENSO, drought, and heat waves have pushed the Amazon's water cycle into a state of crisis as if we had already reached or exceeded the critical threshold.

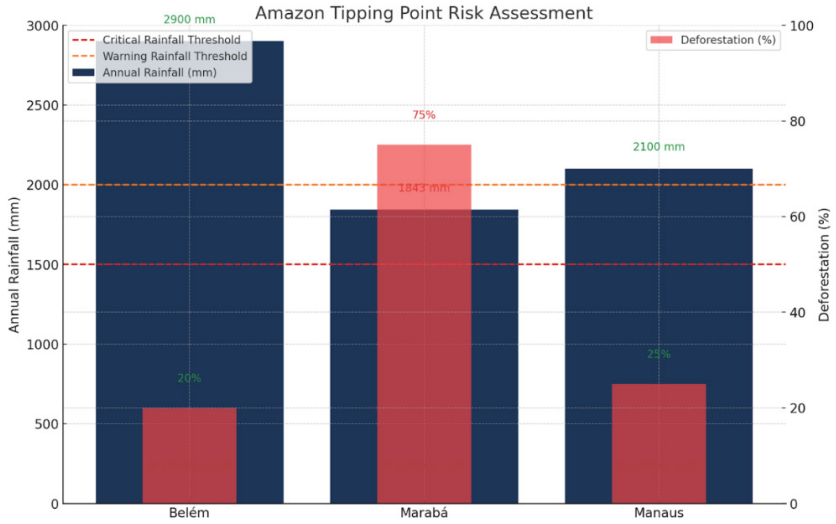

Figure 18. Forest Loss (%) and Evapotranspiration (ET) (mm/year) with Critical Thresholds.

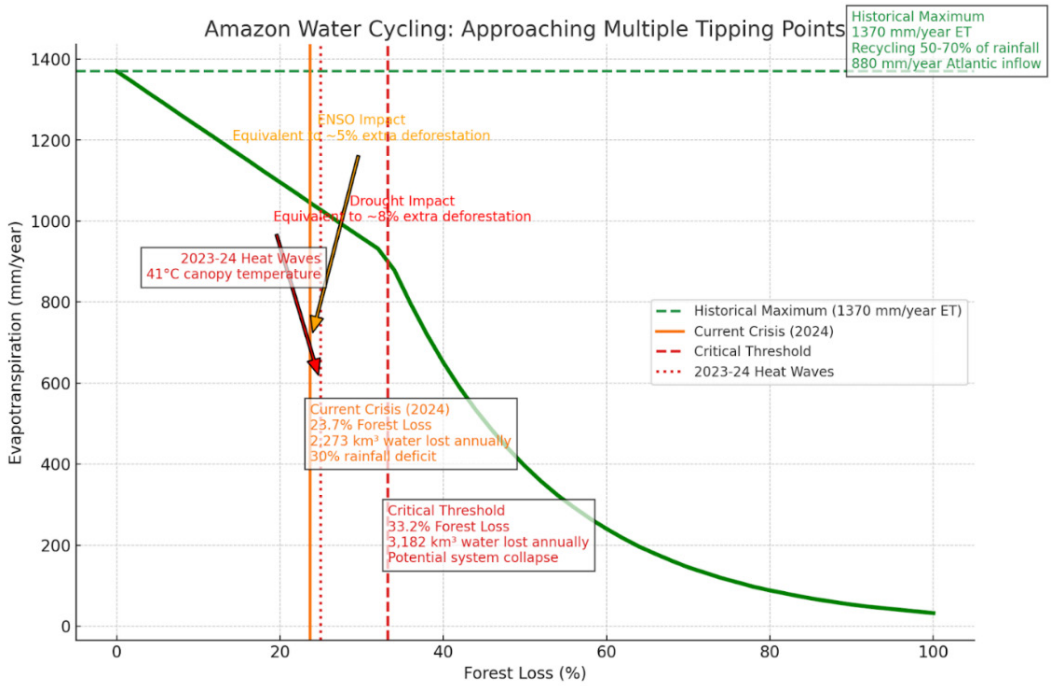

Figure 19. The Shifting Rainfall Distribution Across Belém, Marabá, and Manaus.

This graph underscores that the Amazon is not just losing trees—it's losing time. Climate extremes are eroding the resilience buffer faster than deforestation statistics alone can capture.

Figure 19 shows the shifting rainfall distribution across Belém, Marabá, and Manaus, which are key locations along the Amazon's Biotic Pump Pathway. It is that pathway which drives moisture from the Atlantic Ocean deep into the rainforest.

3.7. Rainfall Distribution Patterns: Annual Dry vs. Rainy Days Along the Biotic Pump Pathway

Belém, closest to the coast, experiences the highest number of rainy days with fewer dry days, reflecting its strong connection to Atlantic moisture. Moving inland to Marabá, the pattern shifts dramatically—dry days increase significantly, and rainy days decrease, highlighting the disruptive impact of deforestation and land degradation on the biotic pump's efficiency. Despite Marabá's proximity to the coast, its rainfall is irregular, with fewer rainy days but higher intensity during those events, indicating climate stress and ecosystem instability. In contrast, Manaus shows a more balanced pattern, similar to Belém, due to the buffering effect of surrounding forest cover, although it's not immune to fluctuations during climate anomalies like ENSO. This uneven distribution—marked by a shift from consistent rainfall to sporadic, intense events—signals a destabilizing hydrological cycle, increasing the risks of prolonged droughts, flash floods, and ecosystem collapse across the Amazon (**Figure 20**).

The following **Figure 21** shows the fundamental differences between the three regions of the Brazilian Amazon.

3.8. Amazon Rainfall & Deforestation: State of Pará – Marabá Region

This graphic illustrates the rainfall pattern along the biotic pump pathway, stretching from the Atlantic coast to the Amazon interior, focusing on the State of Pará and particularly the Marabá region. The black line represents the theoretical intact forest scenario, where rainfall remains consistently high (~2900 mm/year) without the impacts of deforestation. In contrast, the orange curve shows the hypothetical "no recycling" scenario, where deforestation and land degradation completely disrupt the Amazon's ability to recycle moisture, causing a sharp decline in rainfall as we move inland.

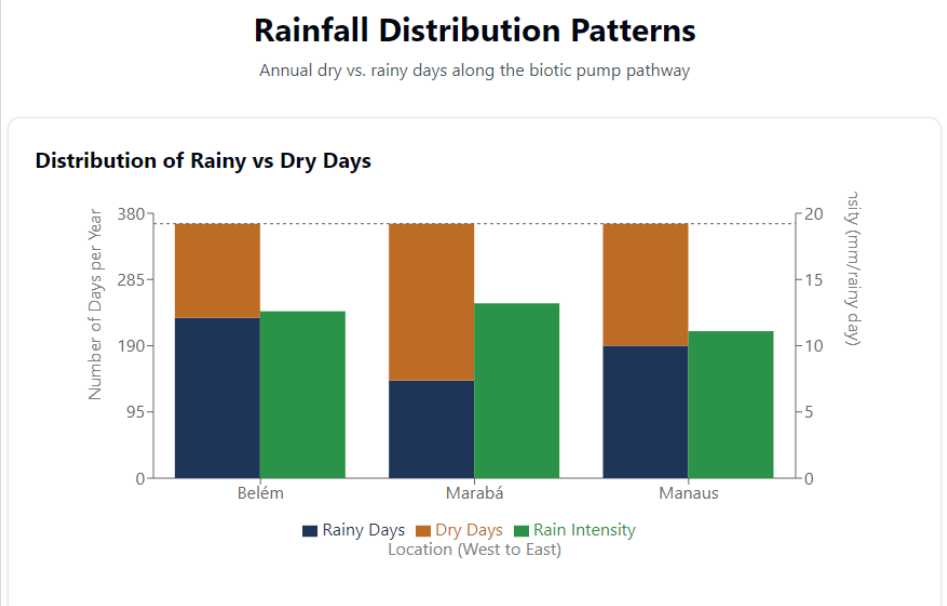

Figure 20. Comparison of Rainforest Conditions on Rainy Versus Dry Days.

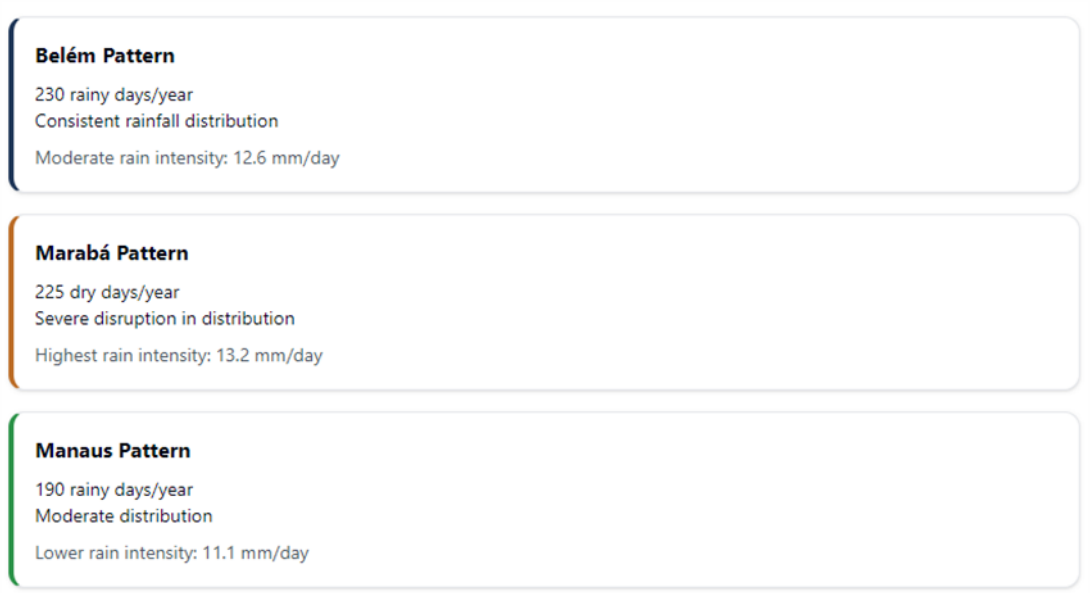

Figure 21. Regional rainfall patterns.

The current state, depicted by the green line with data points, reflects the actual observed rainfall patterns. Notably:

- Belém, with 20% deforestation, maintains high rainfall (~2900 mm/year) due to its coastal proximity and relatively intact moisture recycling capacity.
- Marabá, however, shows a stark contrast. Despite being closer to the coast than Manaus, its rainfall has dropped to 1843 mm/year, heavily impacted by 75% deforestation. This places Marabá in the "critical deforestation zone," where the landscape struggles to retain moisture, pushing rainfall dangerously close to the 2000 mm warning threshold and approaching the 1500 mm critical threshold, beyond which ecosystems face irreversible damage.
- Manaus, further inland with 25% deforestation, surprisingly maintains higher rainfall (~2100 mm/year) than Marabá. This resilience is due to the

surrounding forest still playing a significant role in moisture recycling, although it remains vulnerable to future deforestation and climate stressors.

The key takeaway is that deforestation's impact on rainfall is not linear. Regions like Marabá demonstrate that once a critical tipping point is crossed, rainfall declines rapidly, even if nearby regions remain relatively intact. This underscores the fragile balance of the Amazon's climate system—degradation along the biotic pump pathway weakens the entire system, affecting areas far beyond where deforestation occurs.

Figure 22 indicates that 1800 mm annual precipitation is the threshold point for maintaining a viable rainforest ecosystem.

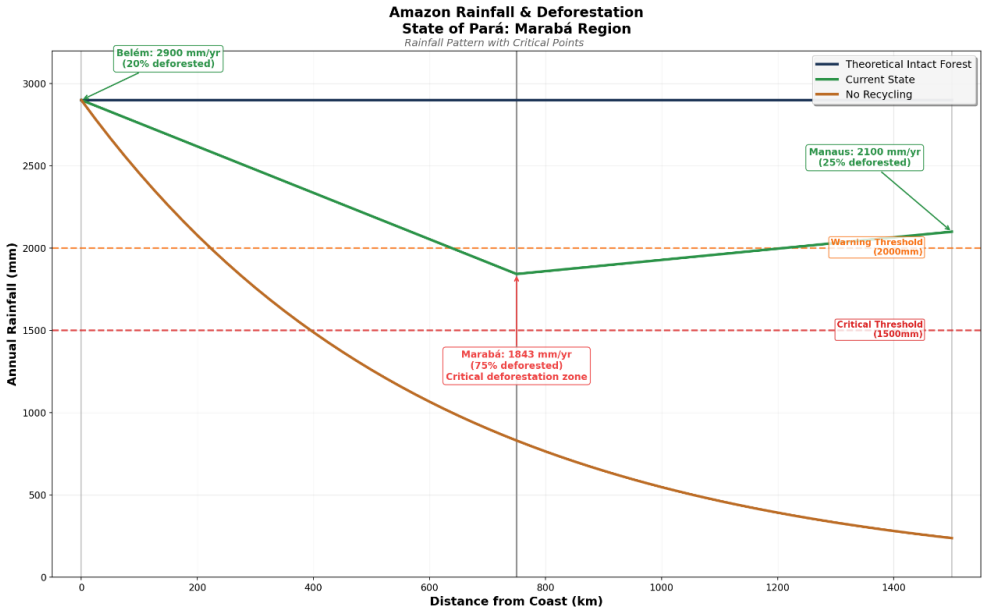

Figure 22. The Danger Points Beyond Which the Biotic Pump No Longer Functions.

3.9. Pará State Deforestation Context

Deforestation varies across the state:

- 20–30%: Coastal and preserved areas
- 50%: State average
- 75%: Heavily impacted regions (including Marabá)

Marabá sits in one of the most heavily deforested regions, part of the "Arc of Deforestation"

This severe forest loss explains the significant drop in rainfall and disruption of the biotic pump.

4. Discussion

As shown by Andrew Felton *et al.*, above-ground vegetation, by means of evapotranspiration is responsible for a significant flow of water from rainfall to humid soil and then, out through the plant stomata back into the atmosphere [31]. Felton et al. give mean transit times of water from ~5 days in croplands to ~18 days in evergreen needleleaf forests, with a global median of 8.1 days [31]. The experiments we have recently carried out verify the contribution of vegetation to the hydrological cycle and the substantial flow of water which then ensues.

Bunyard refers to his studies of 2012 on surface humidity (84 m above sea-level) as obtained from radiosonde balloons released from sites along the path of the Africa to South America Trade Winds [17]. The evaporative force, f_E, as calculated using the physics of Makarieva/Goschkov [1,2], indicates the partial pressure force of water vapour to move the air upwards towards cloud-forming altitudes. In **Figure 23** below, we see the results averaged out for January 2012, from measurements of meteorological data obtained in the early morning release of the balloons. The highest f_E and the highest surface humidity in grams per cubic metre is for Leticia in the Colombian Amazon followed by other Amazon sites and crossing the Atlantic Ocean to the desert of the Sahara.

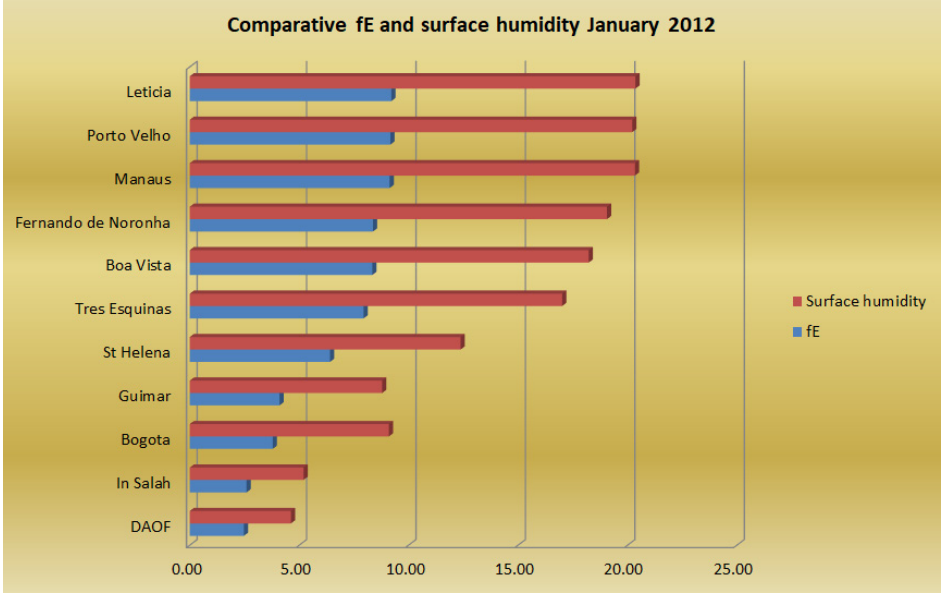

Figure 23. Surface Data at 84 Metres, Collected from Radiosonde Balloons Launched at Locations Aligned with Trade Winds Between North Africa and South America.

Note: f_E is the Evaporative Force Derived from Evapotranspiration.

Experiments such as that of 22nd May, 2025, (**Figures 12** and **13**), give results for average absolute humidity of grass at 20 grams per cubic metre which conforms to that measured for Leticia, Colombia. The control meanwhile, with 12 grams humidity per cubic metre, is similar to that of the South Atlantic Island of St Helena, over which the Trade Winds pass. The indications are that our experiments are wholly consistent with general meteorological data.

With regards to the re-evaluation of experiments on the relationship between the rate of condensation and airflow, (**Figures 1** to **7**), we provide evidence that the physics underpinning the biotic pump should be taken into account when considering the hydrological and climate consequences of deforestation, especially in the equatorial tropics. We find from the physics of condensation that the ratio of 0.17/2.5 of latent heat is equivalent to the kinetic energy associated with partial pressure change when condensation takers place, hence the latent heat ratio. In effect, that ratio allows us to determine the airflow velocity once we know the rate of rainfall in an event such as a hurricane.

5. Conclusion

Already deforestation is affecting the biotic pump and, together with global warming and anthropogenic climate change, we can determine that, once rainfall annually reduces to below 1800 mm, forest degradation will result. Marabá, in Brazil's eastern Amazon, already shows signs that the biotic pump is impaired. In part, at least, the Amazon droughts of 2023/2024 can be explained by a misfunctioning of the biotic pump.

Finally, for those hydrologists and climatologists who still doubt the significance of the implosion energy from water vapour condensation on climate systems and who disregard the biotic pump in their modelling of climate processes, we refer to the Newcomen atmospheric steam engine, invented three centuries ago.

This understanding has significant implications for climate models. The failure to incorporate biotic pump dynamics into General Circulation Models risks underes-t imating the effects of deforestation on rainfall. As dem-o nstrated in the Amazon Basin, widespread deforestation weakens the pressure gradients that sustain trade winds, leading to severe aridification. Just as the New-comen engi ne halts without proper heat removal, atmos-pheric circul ation falters when forests are unable to main-tain the biotic pump.

Investing in forests means investing in the planet's climate regulation system. By preserving the Amazon and other major forest biomes, we ensure the continuity of fly-

ing rivers, these vast atmospheric moisture streams driven by the biotic pump, that sustain agriculture, stabilize regional climates, and help cool the planet.

Teleconnections between forest regions, such as from the Congo Basin to the Amazon, play a crucial role in maintaining rainfall patterns across continents. There is growing evidence that Amazon-generated moisture extends far beyond South America, including all the way to Southern Africa and crossing the Caribbean and potentially contributing to the reactivation of the biotic pump over parts of Central America and the American Midwest.

In conclusion, the restoration of ecosystems, with their soils and plant-life, will be the most effective way to cool the planet and stabilize the climate. Increasingly, we are coming to realise the crucial role that water cycles, including those engendered by the biotic pump, play in stabilising climate and its generation of weather patterns. Simultaneously, as healthy ecosystems are regenerated, atmospheric carbon will be sequestered in new living biomass, thereby helping to cool the Earth by means of a reduction in greenhouse gases at the Earth's surface. In effect, when we repair the biosphere, the Earth can once again regulate its own temperature.

Ecological restoration, carried out by people everywhere, is our fastest path out of climate chaos. Cooling the planet with plants, especially tropical rainforests which, through massive evapotranspiration, are the Earth's most powerful cooling agent, not only lowers temperatures but also brings more rain across continents and enhances the uptake of carbon dioxide by a growing biomass. By working together to restore soils and ecosystems, we can turn this emerging new reality of what are the prime climate-forming agents into real action. But we must act fast. Once we pass the tipping points in the Earth's climate system, the planet's climate will cascade into a new state, incompatible with large scale human societies.

Author Contributions

All authors have read and agreed to the published version of the manuscript.

Peter Bunyard developed and designed the methodology for studying the airflow dynamics resulting from water vapour condensation. He also carried out all the experiments listed in the paper, both for research on the physics of the biotic pump and for measuring the cooling characteristics of vegetation.

Ali Bin Shahid undertook the evaluation of the implications of deforestation on the biotic pump with reference to the Amazon Basin. He has also developed methods to evaluate the temperature regulation by vegetation and to test for it being proactive.

Rob de Laet has contributed his ideas for undertaking the experimentation and has played an invaluable role in his conceptualisation of ways to tackle global warming by means of ecosystem restoration.

Funding

This work received no external funding.

Institutional Review Board Statement

Not applicable.

Informed Consent Statement

Not applicable.

Data Availability Statement

If required the experimental results as described would be available by contacting Peter Bunyard, email: peter.bunyard@btinternet.com

Acknowledgments

With acknowledgment of the support provided by the Sensory Trust, St Austell, Cornwall, UK, which sponsored the undertaking of the recent cooling experiments of vegetation.

Conflicts of Interest

The authors declare no conflict of interest.

References

[1] Makarieva, A., Gorshkov, V., 2007. Biotic pump of atmospheric moisture as driver of the hydrological cycle on land. Hydrology and Earth System Sciences. 11, 1013–1033. DOI: https://doi.org/10.5194/hess-11-1013-2007

[2] Makarieva, A., Gorshkov, V., 2009. Reply to A. G.

C. A. Meesters et al.'s comment on "Biotic pump of atmospheric moisture as driver of the hydrological cycle on land". Hydrology and Earth System Sciences. 13, 1307–1311. DOI: https://doi.org/10.5194/hess-13-1307-2009

[3] Bunyard, P.P., Collin, E., de Laet, R., et al., 2024. Restoring the earth's damaged temperature regulation is the fastest way out of the climate crisis. Cooling the planet with plants. International Journal of Biosensors and Bioelectronics. 9(1), 7–15. DOI: https://doi.org/10.15406/ijbsbe.2024.09.00237

[4] Rolt, L.T.C., Allen, J.S., 1977. The Steam Engine of Thomas Newcomen. Moorland: Hartington, UK. pp. 160.

[5] Bunyard, P.P., de Laet, R., 2024. Cooling the Climate: How to Revive the Biosphere and Cool the Earth within 20 Years. Ethics International Press: Cambridge, UK.

[6] Salati, E., 1987. The forest and the hydrological cycle. In: Dickinson, R. (ed.). Geophysiology of Amazonia. Wiley: New York, USA. pp. 273–296.

[7] Rocha, D.G., et al., 2023. Habitat use patterns suggest that climate-driven vegetation changes will negatively impact mammal communities in the Amazon. Animal Conservation. 26(5), 663–674. DOI: https://doi.org/10.1111/acv.12853

[8] Anadón, J.D., Sala, O.E., Maestre, F.T., 2014. Climate change will increase savannas at the expense of forests and treeless vegetation in tropical and subtropical Americas. Journal of Ecology. 102, 1363–1373. DOI: https://doi.org/10.1111/1365-2745.12325

[9] Ban-Weiss, G.A., Bala, G., Cao, L., et al., 2011. Climate forcing and response to idealized changes in surface latent and sensible heat. Environmental Research Letters. 6(3), 034032. DOI: https://doi.org/10.1088/1748-9326/6/3/034032

[10] Bunyard, P.P., 2015. The Biotic Pump We Ignore At Our Peril. Resurgence & Ecologist. 290. Available from: https://www.resurgence.org/magazine/article4423-the-biotic-pump-we-ignore-at-our-peril.html (cited 25 January 2025).

[11] Marengo, J.A., 2006. On the hydrological cycle of the amazon basin: A historical review and current state-of-the-art. Revista brasileira de meteorologia. 21, 1–19.

[12] Makarieva, A.M., Gorshkov, V.G., Sheil, D., et al., 2013. Where do winds come from? A new theory on how water vapor condensation influences atmospheric pressure and dynamics. Atmospheric Chemistry and Physics. 13, 1039–1056. DOI: https://doi.org/10.5194/acp-13-1039-2013

[13] Makarieva, A.M., Gorshkov, V.G., Sheil, D., et al., 2014. Why does air passage over forest yield more rain? Examining the coupling between rainfall, pressure and atmospheric moisture content. Journal of Hydrometeorology. 15(1), 411–426. DOI: https://doi.org/10.1175/JHM-D-12-0190.1

[14] Spracklen, D.V., Arnold, S.R., Taylor, C.M., 2012. Observations of increased tropical rainfall preceded by air passage over forests. Nature. 489, 282–285. DOI: https://doi.org/10.1038/nature11390

[15] Bunyard, P.P., Hodnett, M., Pena, C., et al., 2017. Condensation and partial pressure change as a major cause of airflow: experimental evidence. Revista DYNA. 84(202), 92–101.

[16] Bunyard, P.P., Hodnett, M., Pena, C., et al., 2019. Further experimental evidence that condensation is a major cause of airflow. Revista DYNA. 86(209), 56–63.

[17] Bunyard, P.P., 2014. How the Biotic Pump links the hydrological cycle and the rainforest to climate: Is it for real? How can we prove it?. Instituto de Estudios y Servicios Ambientales-IDEASA: Bogotá, Colombia. pp. 114.

[18] Daniels, F., Williams, J., 1966. Physical Chemistry, International Edition. John Wiley and Sons: New York, USA.

[19] McIlveen, R., 2010. Fundamentals of weather and climate, 2nd ed. Oxford University Press: Oxford, UK.

[20] Bunyard, P.P., de Laet, R., 2024. Restore ecosystems to cool the climate. In: Lackner, M., et al. (eds.). Handbook of Climate Change Mitigation and Adaptation. Springer: New York, USA. pp. 1–28. DOI: https://doi.org/10.1007/978-1-4614-6431-0_206-1

[21] Bunyard, P.P., de Laet, R., 2024. Cooling the Climate: How to revive the Biosphere and cool the Earth within 20 years. Ethics International Press: Cambridge, UK.

[22] Hodnett, M.G., Oyama, M.D., Tomasella, J., et al., 1996. Comparisons of long-term soil water storage behaviour under pasture and forest in three areas of Amazonia. In: Gash, J., et al. (eds.). Amazonian Deforestation and Climate. John Wiley: Chichester, UK. pp. 57–77.

[23] Harde, H., 2013. Radiation and Heat Transfer in the Atmosphere: A Comprehensive Approach on a Molecular Basis. International Journal of Atmospheric Sciences. 2013, 503727. DOI: https://doi.org/10.1155/2013/503727

[24] Boyce, C.K., Lee, J.E., Field, T.S., et al., 2010. Angiosperms helped put the rain in the rainforests: the impact of plant physiological evolution on tropical biodiversity. Annals of the Missouri Botanical Garden. 97(4), 527–540. DOI: https://doi.org/10.3417/2009143

[25] Benton, M.J., Wilf, P., Sauquet, H., 2022. The Angiosperm Terrestrial Revolution and the origins of modern biodiversity. New Phytologist. 233(5), 2017–2035. DOI: https://doi.org/10.1111/nph.17822

[26] Barrett, P., 1999. Antarctic climate history over the

last 100 million years. Terra Antarctica Reports. 3, 43–72.

[27] Pagani, M., Zachos, J.C., Freeman, K.H., et al., 2005. Marked Decline in Atmospheric Carbon Dioxide Concentrations During the Paleogene. Science. 309(5734), 600–603. DOI: https://doi.org/10.1126/science.1110063

[28] Koch, A., Brierly, C., Maslin, M.M., et al., 2019. Earth system impacts of the European arrival and Great Dying in the Americas after 1492. Quaternary Science Reviews. 207, 13–36.

[29] Wu, Y., Wen, B., Ye, T., et al., 2025. Estimating the urban heat-related mortality burden due to greenness: a global modelling study. Lancet Planetary Health. 1–12. DOI: https://doi.org/10.1016/S2542-5196(25)00062-2

[30] Marull, Y., 2012. Amazon's flying water vapor rivers bring rain to Brazil. Phys.org. Available from: https://phys.org/news/2012-09-amazon-vapor-rivers-brazil.html (cited 13 November 2014).

[31] Felton, A.J., Fisher, J.B., Hufkens, K., et al., 2025. Global estimates of the storage and transit time of water through vegetation. Nature Water. 3, 59–69. DOI: https://doi.org/10.1038/s44221-024-00365-9